YMTHE, Volume *32*

Supplemental Information

Immunosuppressant therapy averts rejection of allogeneic *FKBP1A*-disrupted CAR-T cells

Colby R. Maldini, Angelica C. Messana, Paula B. Bendet, Adam J. Camblin, Faith M. Musenge, Moriah L. White, Joseph J. Rocha, Lindsey J. Coholan, Cisem Karaca, Frederick Li, Bo Yan, Vladimir D. Vrbanac, Emily Marte, Daniel T. Claiborne, Christian L. Boutwell, and Todd M. Allen

Figure S1

A

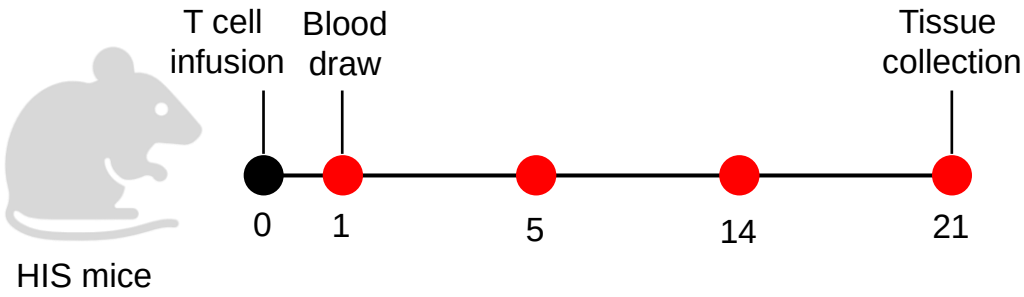

	HLA-I					
T cell donor	A_1	A_2	B_1	B_2	C_1	C_2
Syngeneic	02:01	30:02	18:01	45:01	05:01	16:01
Allogeneic	01:01	31:01	08:01	15:17	07:01	07:01

B

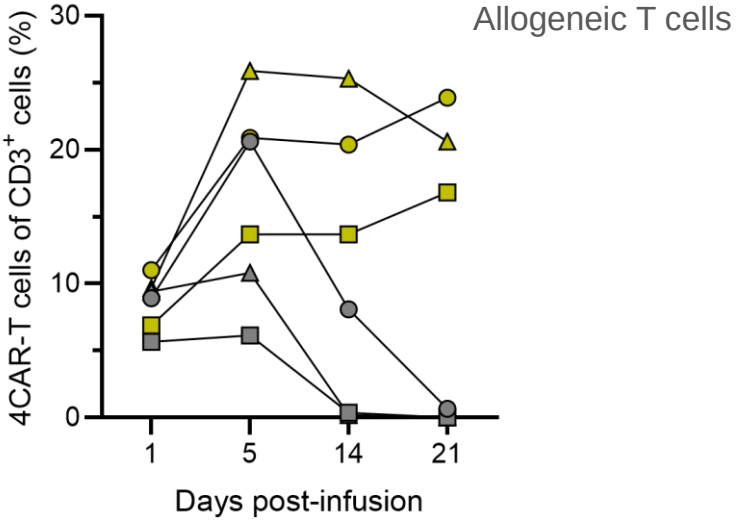

C

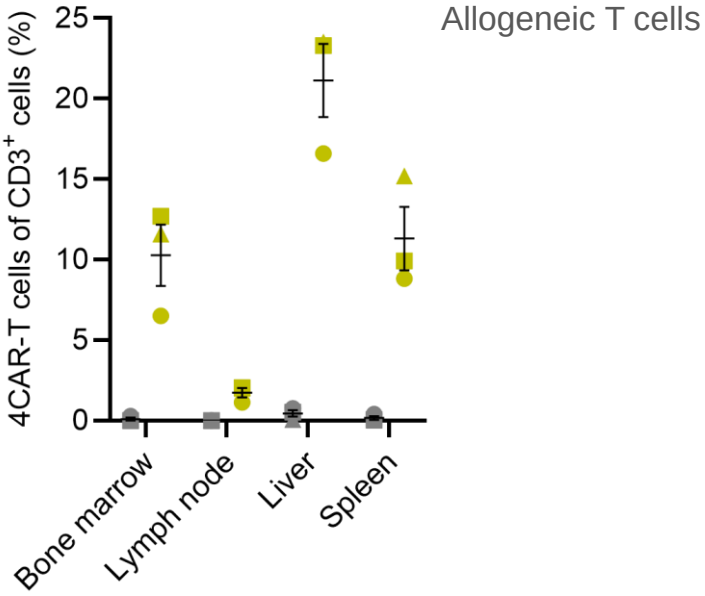

HIS mice reject HLA-mismatched 4CAR-T cells. A Human immune system (HIS) mice (BLT-NSG; n = 3) were infused with 5 x 10^6 CD4-based CAR-T cells (4CAR) of each type derived from a syngeneic HIS mouse donor and an allogeneic HLA-mismatched human donor. **B,C** Longitudinal frequency of 4CAR-T cells in circulation (**B**) and in resected tissues at 3-weeks post-infusion (**C**)**.** For all data, symbols represent individual mice, lines indicate mean and error bars show ±s.e.m.

Figure S2

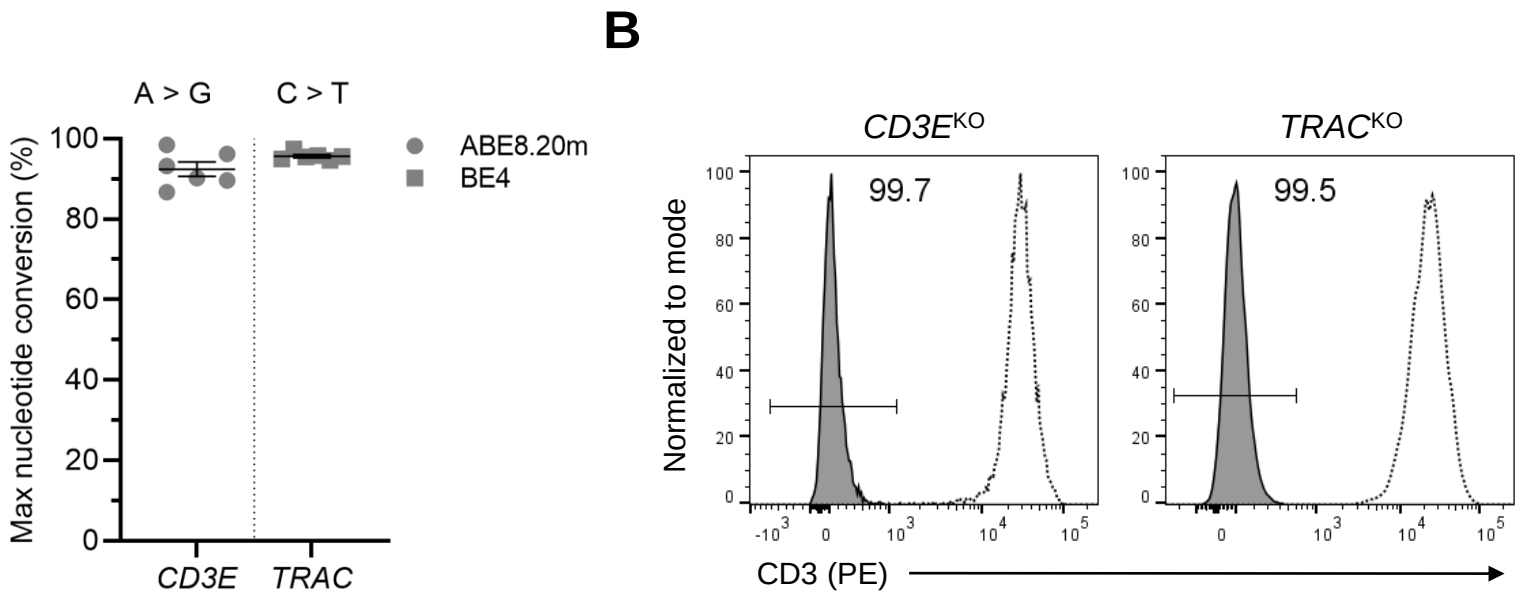

Disruption of *CD3E and TRAC* abrogates T cell receptor surface expression. Human T cells were electroporated with a *CD3E*- or *TRAC*-specific sgRNA complexed with mRNA encoding ABE8.20m or BE4, respectively. **A** Frequency of nucleotide conversion determined by next-generation sequencing in T cells 5-days post-electroporation. Symbols are independent donors. Lines represent mean and error bars show ±s.e.m. **B** Histograms indicate CD3 protein surface expression in base-edited (gray) and unmodified (white) T cells.

Figure S3

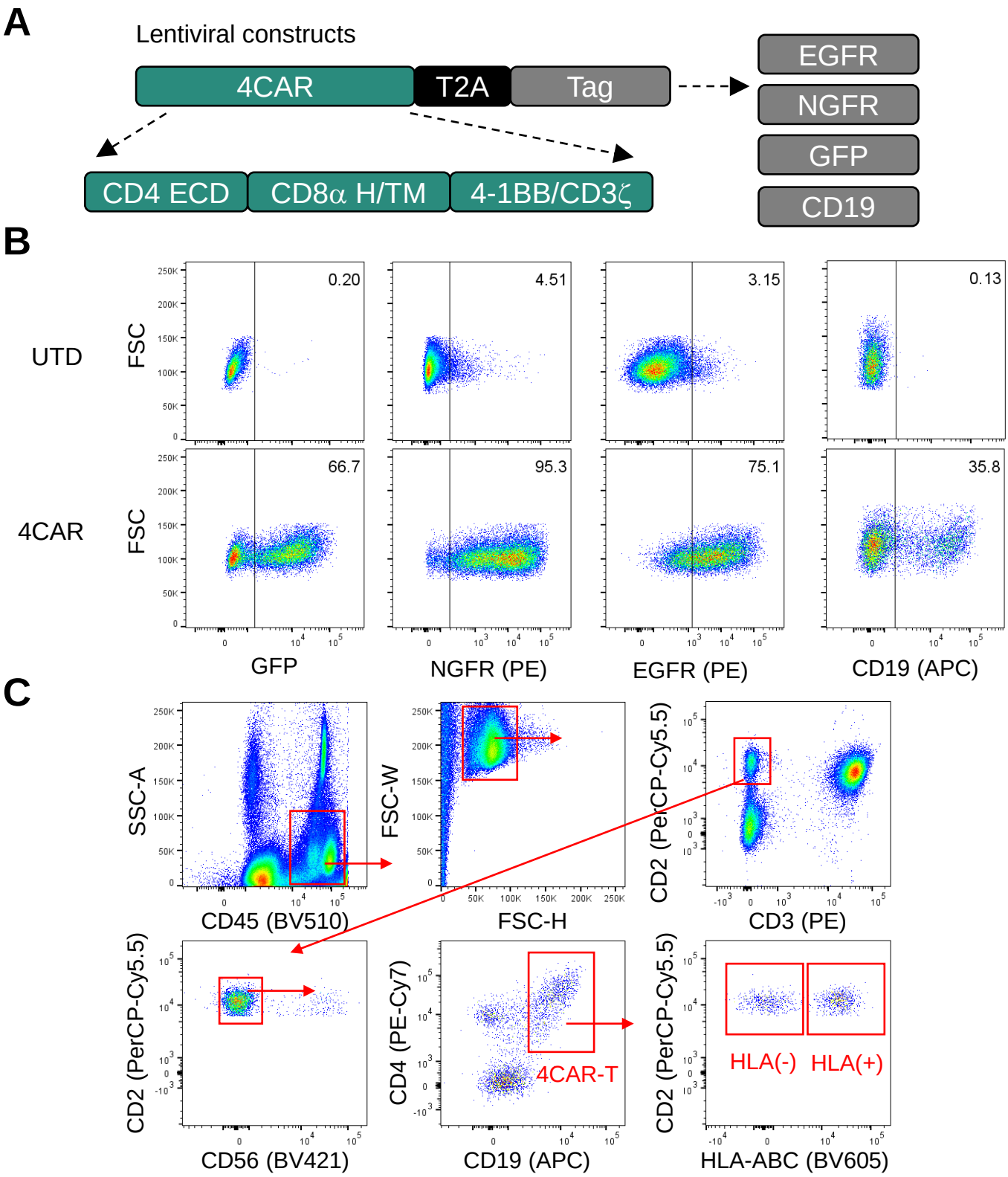

CD4-based CAR-T cell generation and *ex vivo* identification by flow cytometry. A Schematic of lentiviral constructs used to generate CD4-based CAR-T cells. CD4-based CAR (4CAR) consists of the CD4 extracellular domain (ECD) fused to the CD8α hinge (H) and transmembrane (TM) regions along with the intracellular 4-1BB and CD3ζ activating motifs. 4CAR was separated by an intervening T2A self-cleaving peptide to a molecular tag comprising GFP or truncated EGFR, NGFR or CD19. **B** FACS plots indicate frequency of transduced 4CAR-T cells expressing the indicated molecular tag incorporated into the 4CAR lentiviral construct. Untransduced (UTD) T cells were used as a negative control. **C** Representative flow cytometry gating strategy to identify HLA^{+} and HLA-deficient 4CAR-T cells from whole blood or tissue of HIS mice.

Figure S4

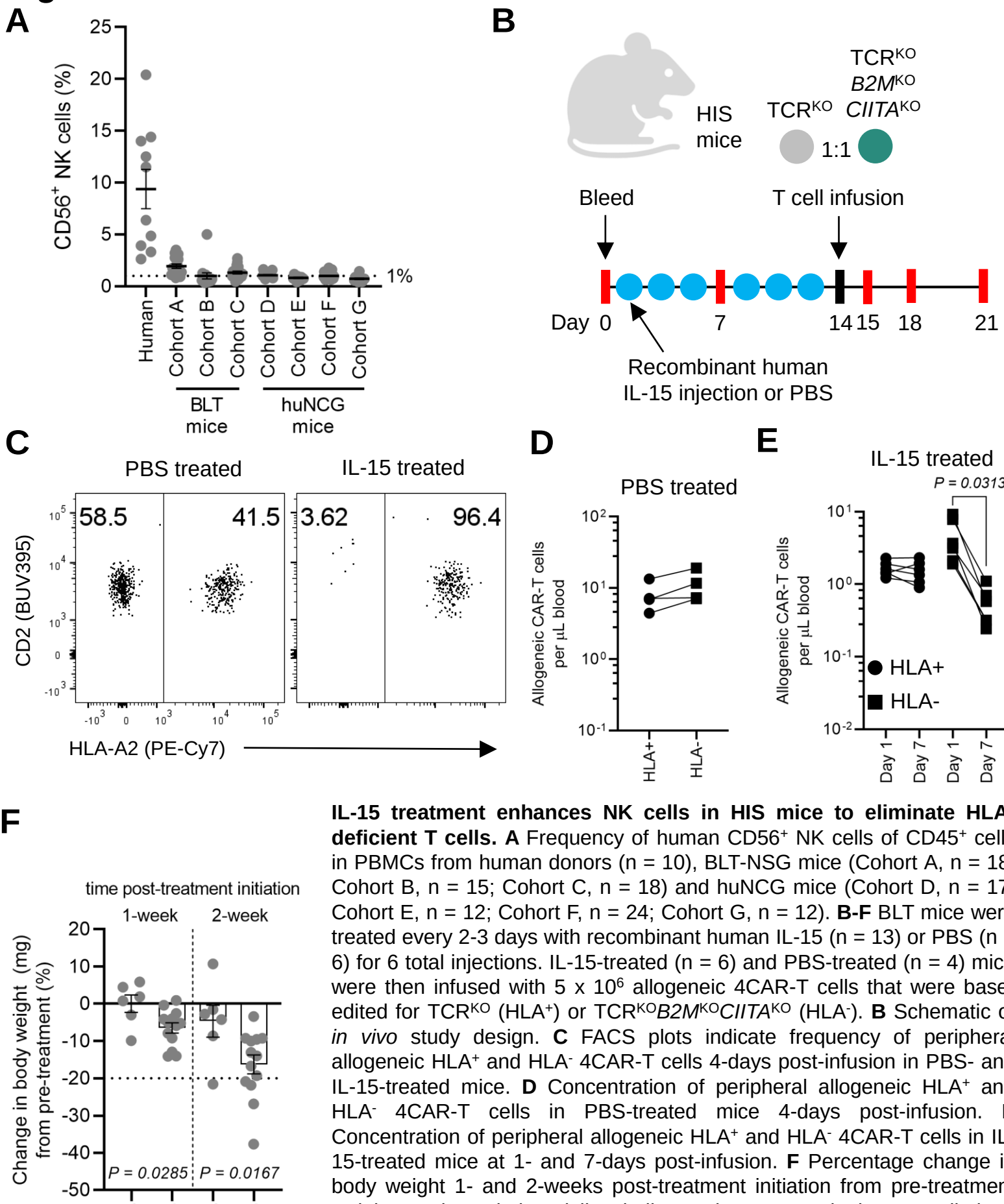

IL-15 treatment enhances NK cells in HIS mice to eliminate HLA-deficient T cells. A Frequency of human CD56$^+$ NK cells of CD45$^+$ cells in PBMCs from human donors (n = 10), BLT-NSG mice (Cohort A, n = 18; Cohort B, n = 15; Cohort C, n = 18) and huNCG mice (Cohort D, n = 17; Cohort E, n = 12; Cohort F, n = 24; Cohort G, n = 12). **B-F** BLT mice were treated every 2-3 days with recombinant human IL-15 (n = 13) or PBS (n = 6) for 6 total injections. IL-15-treated (n = 6) and PBS-treated (n = 4) mice were then infused with 5 x 10^6 allogeneic 4CAR-T cells that were base-edited for TCR^{KO} (HLA$^+$) or TCR^{KO}*B2M*^{KO}*CIITA*^{KO} (HLA$^-$). **B** Schematic of *in vivo* study design. **C** FACS plots indicate frequency of peripheral allogeneic HLA$^+$ and HLA$^-$ 4CAR-T cells 4-days post-infusion in PBS- and IL-15-treated mice. **D** Concentration of peripheral allogeneic HLA$^+$ and HLA$^-$ 4CAR-T cells in PBS-treated mice 4-days post-infusion. **E** Concentration of peripheral allogeneic HLA$^+$ and HLA$^-$ 4CAR-T cells in IL-15-treated mice at 1- and 7-days post-infusion. **F** Percentage change in body weight 1- and 2-weeks post-treatment initiation from pre-treatment weight. Horizontal dotted line indicates humane endpoint. For all data, symbols indicate biologically independent samples. Statistical significance was calculated by Wilcoxon matched-pairs signed rank test (**E**), and Wilcoxon rank sum test (**F**).

Figure S5

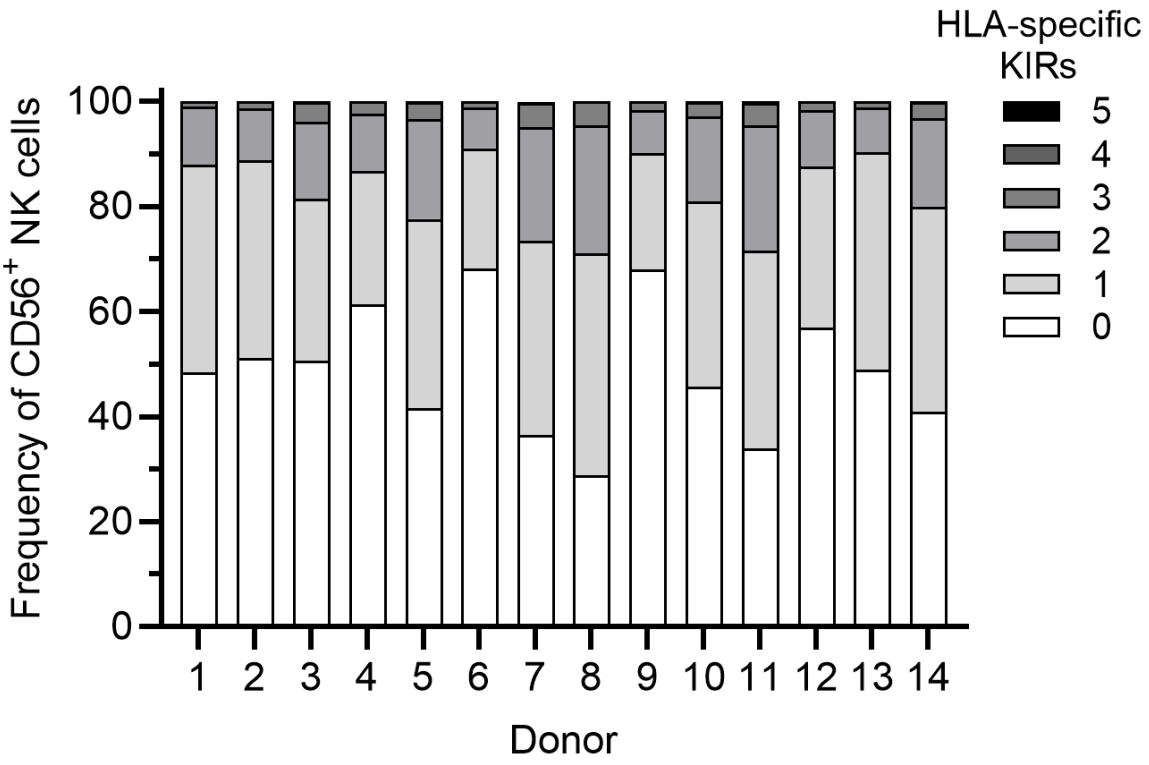

Peripheral blood NK cells express a heterogenous pattern of HLA-specific inhibitory KIRs. Inhibitory KIR expression profile for combinatorial subsets of $CD56^+$ NK cells expressing 0 to 5 KIRs, including KIR2DL1, KIR2DL2/L3, KIR3DL1, KIR2DL4 and KIR2DL5. Data represents 14 independent human donors.

Figure S6

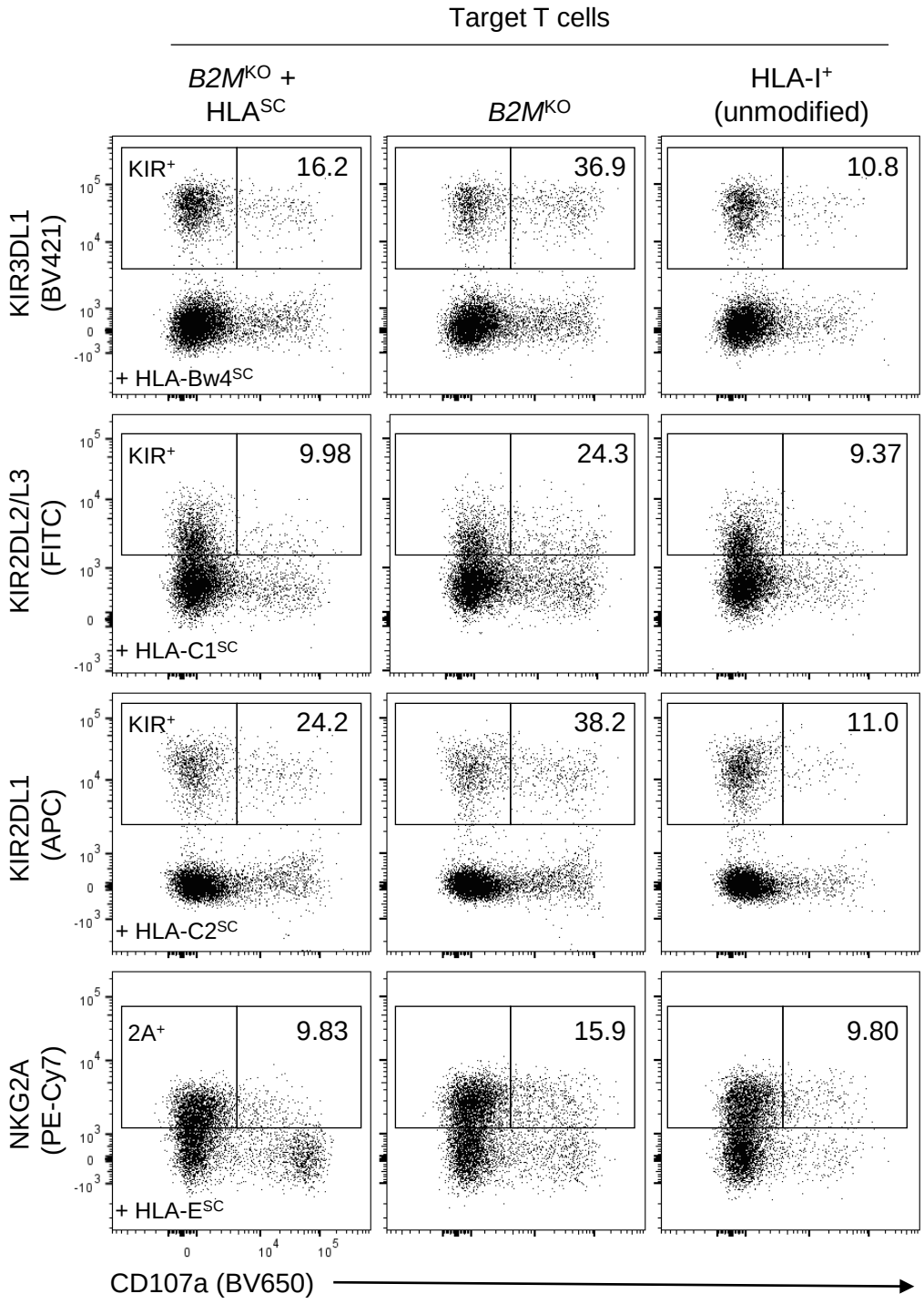

HLA-I deficient T cells expressing an HLA^{SC} molecule inhibit NK cells expressing the corresponding inhibitory receptor. NK cells were stimulated with allogeneic HLA-I^{+} (unmodified) T cells, *B2M*^{KO} T cells, or *B2M*^{KO} T cells engineered to express one HLA^{SC}, either HLA-Bw4^{SC} (HLA-B*57), HLA-C1^{SC} (HLA-C*07:02), HLA-C2^{SC} (HLA-C*04:01), or HLA-E^{SC} (HLA-E*01:03). FACS plots indicate frequency of CD107a^{+} KIRx^{+} or NKG2A^{+} NK cells after stimulation with unmodified T cells, *B2M*^{KO} T cells, or *B2M*^{KO} T cells expressing the HLA^{SC} inhibitory ligand for the corresponding NK cell subset (*i.e.* KIR3DL1-HLA-Bw4^{SC}, KIR2DL2/L3-HLA-C1^{SC}, KIR2DL1-HLA-C2^{SC}, NKG2A-HLA-E^{SC}).

Figure S7

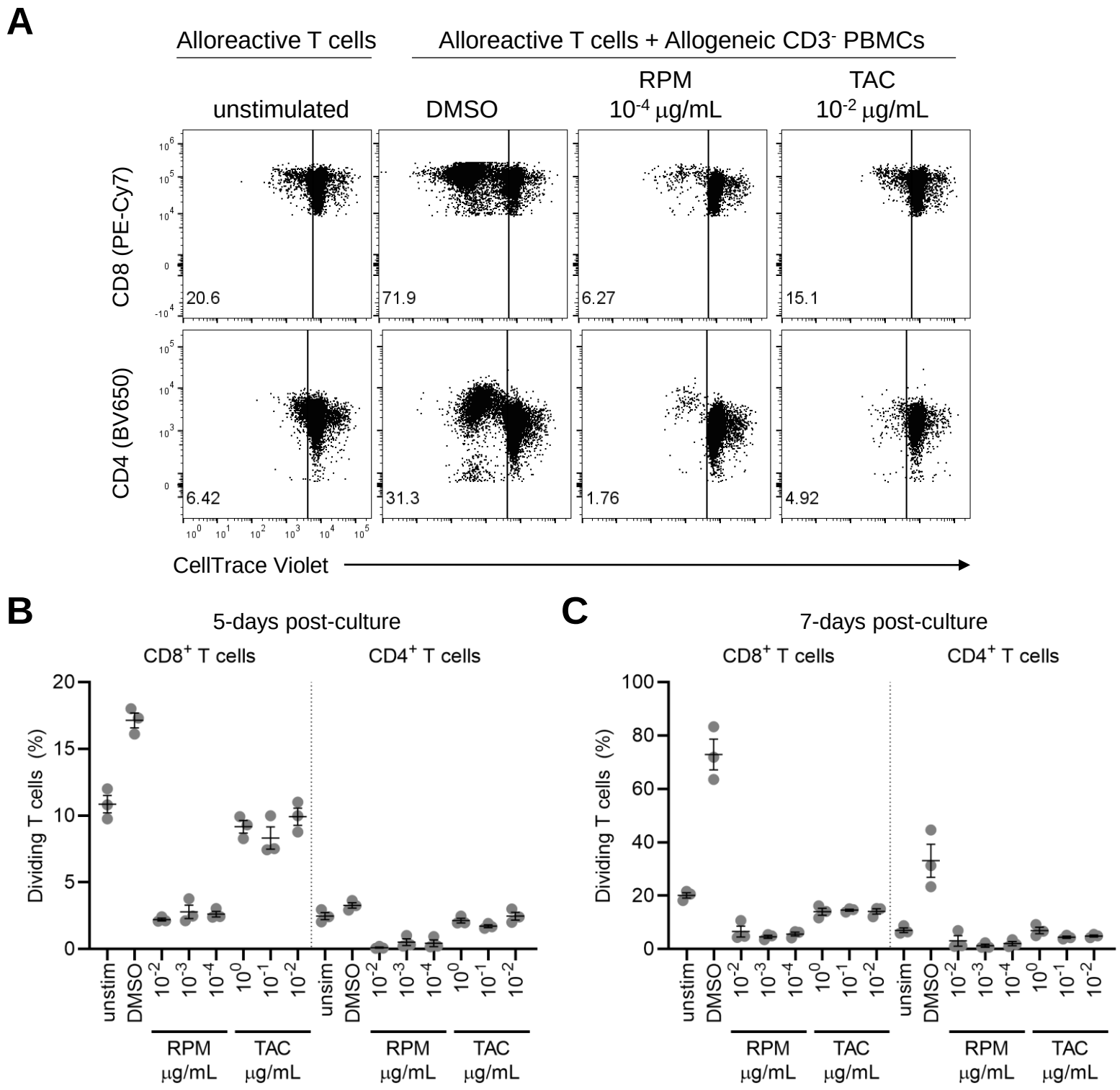

Rapamycin and tacrolimus inhibit *in vitro* priming of alloreactive T cells. Human CD3-depleted PBMCs served as allogeneic target cells to prime CellTrace Violet labeled $CD3^+$ T cells from an HLA-mismatched donor. $CD3^+$ T cells were cultured alone (unstimulated) or in the presence of allogeneic $CD3^-$ PBMCs with DMSO (vehicle), rapamycin (RPM) or tacrolimus (TAC) at different drug concentrations. **A** FACS plots indicate frequency of dividing alloreactive $CD8^+$ and $CD4^+$ T cells 7-days post-culture. **B,C** Frequency of dividing alloreactive $CD8^+$ and $CD4^+$ T cells at 5-days (**B**) and 7-days (**C**) post-culture. Symbols represent independent replicates, lines indicate mean and error bars show ±s.e.m.

Figure S8

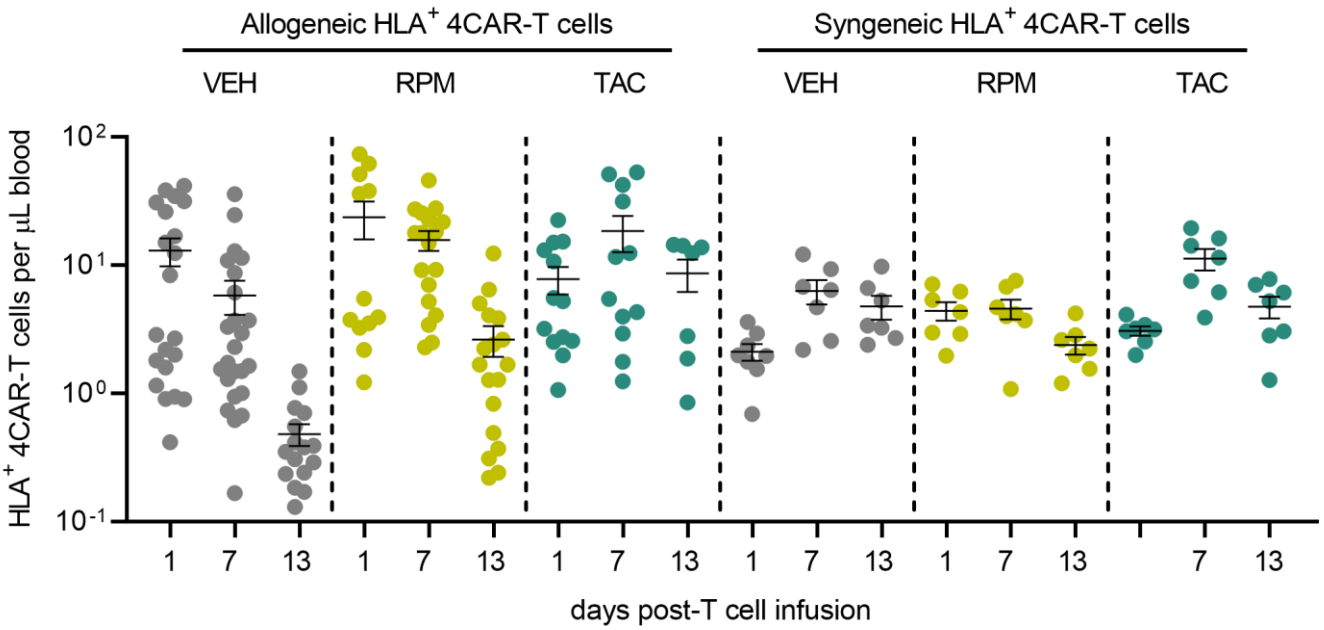

Engraftment of HLA⁺ 4CAR-T cells during drug-treatment interval. Peripheral HLA⁺ 4CAR-T cell concentration in vehicle (VEH), rapamycin (RPM) and tacrolimus (TAC) treated mice measured at 1- and 7- and 13-days post-T cell infusion. Data from allogeneic HLA⁺ 4CAR-T cells represents mice in Cohorts #1 – Cohort #5. Data from syngeneic HLA⁺ 4CAR-T cells represents mice in Cohort #3 and Cohort #4. Symbols represent individual mice, lines indicate mean and error bars show ±s.e.m.

Figure S9

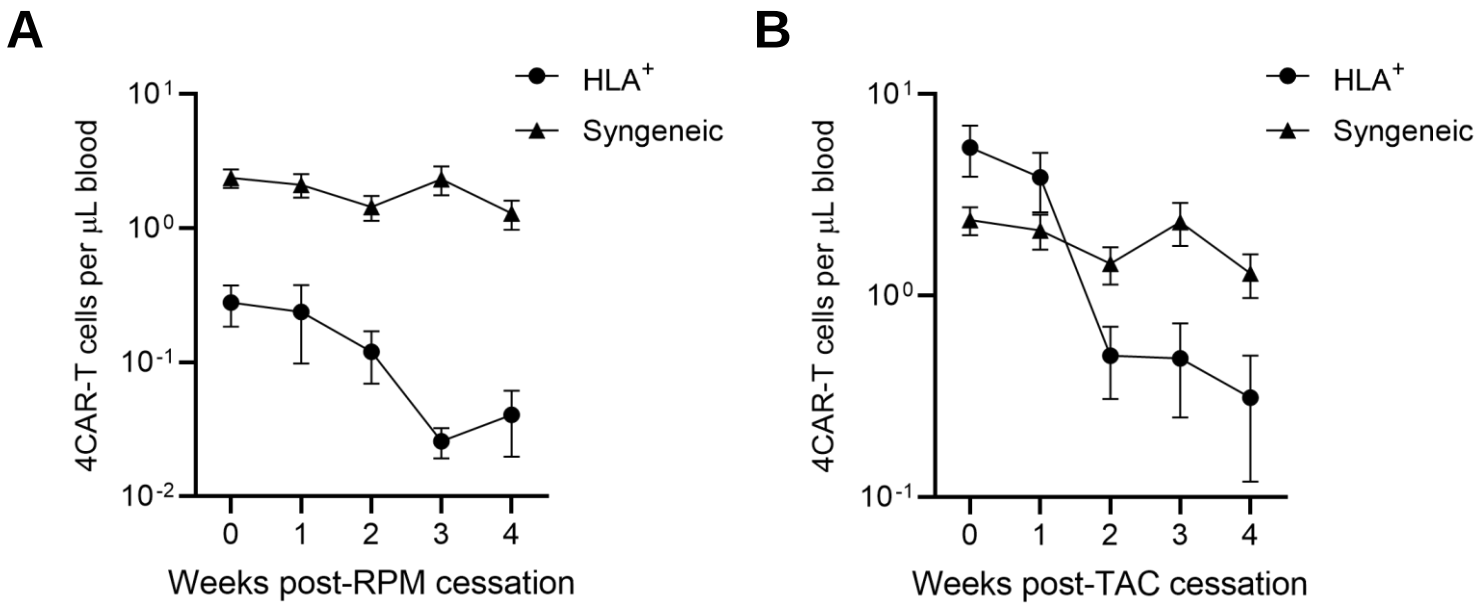

Peripheral allogeneic HLA⁺ 4CAR-T cells are eliminated post-drug treatment withdrawal. huNCG mice from Cohort #3 (n = 4) and Cohort #4 (n = 3) were treated with rapamycin (RPM) or tacrolimus (TAC) daily for 2-weeks. At 1-day post-treatment, 5 x 10^6 allogeneic 4CAR-T cells base-edited for TCR^{KO} (HLA^+) and TCR^{KO}*B2M*^{KO}*CIITA*^{KO} were mixed with 5 x 10^6 syngeneic huNCG mouse-derived 4CAR-T cells and infused into recipient mice. **A,B** Peripheral concentration of allogeneic HLA^+ 4CAR-T cells (circle) and syngeneic 4CAR-T cells (triangle) following RPM (**A**) and TAC (**B**) treatment cessation. Symbols represent mean and errors bars indicate ±s.e.m.

Figure S10

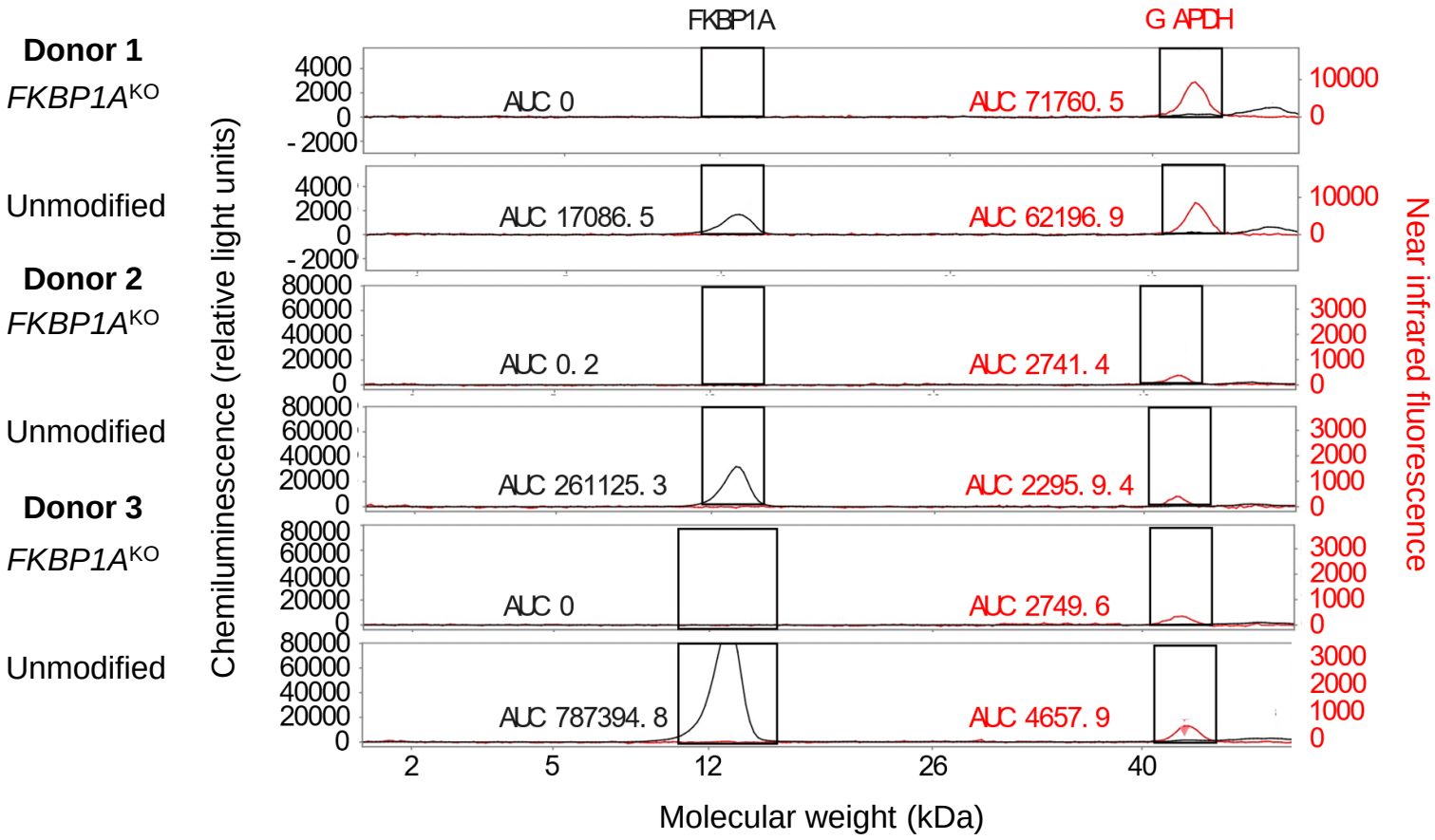

Genetic disruption of *FKBP1A* reduces protein expression. FKBP1A and GAPDH protein detection in unmodified and *FKBP1A*^{KO} T cell lysates from 3 independent donors. Histogram peaks indicate total protein signal from FKBP1A (approximately 12kDa) measured by chemiluminescent fluorescence and GAPDH (approximately 39 kDa) measured by near infrared fluorescence. AUC represents area under the curve of integrated protein signal measured over the indicated ranges (black boxes).

Figure S11

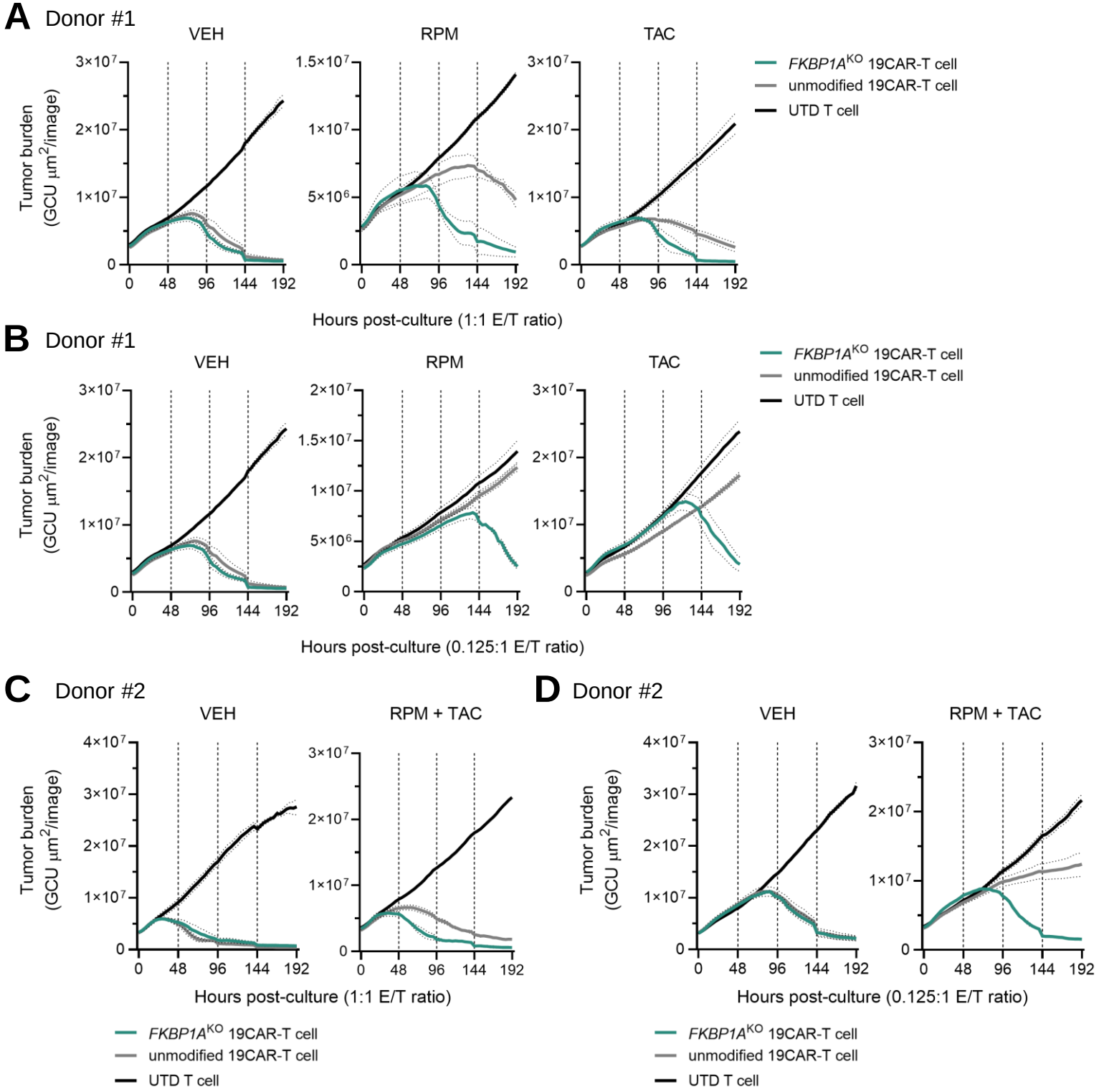

***FKBP1A*^{KO} 19CAR-T cells exhibit *in vitro* anti-tumor cytolytic activity in the presence of rapamycin and tacrolimus.** Incucyte cytotoxicity assay as described in Methods. Tumor burden quantified as Green Calibrated Units (GCU) derived from the fluorescence intensity of GFP^{+} JeKo-1 tumors (targets) cultured in triplicate with effector cells either untransduced (UTD) T cells, unmodified 19CAR-T cells, or *FKBP1A*^{KO} 19CAR-T cells. **A,B** Longitudinal tumor burden at 1:1 (**A**) and 0.125:1 (**B**) effector-to-target (E/T) ratios treated with DMSO vehicle (VEH) control, rapamycin (RPM) or tacrolimus (TAC). **C,D** Longitudinal tumor burden at 1:1 (**C**) and 0.125:1 (**D**) E/T ratios treated with VEH or combination RPM and TAC. Data in **A,B** and **C,D** were generated using independent T cell donors. Bold lines indicate mean GCU from images taken every 4 hours, dotted lines show ±s.e.m., and vertical lines indicate redosing with VEH, RPM and/or TAC.

Figure S12

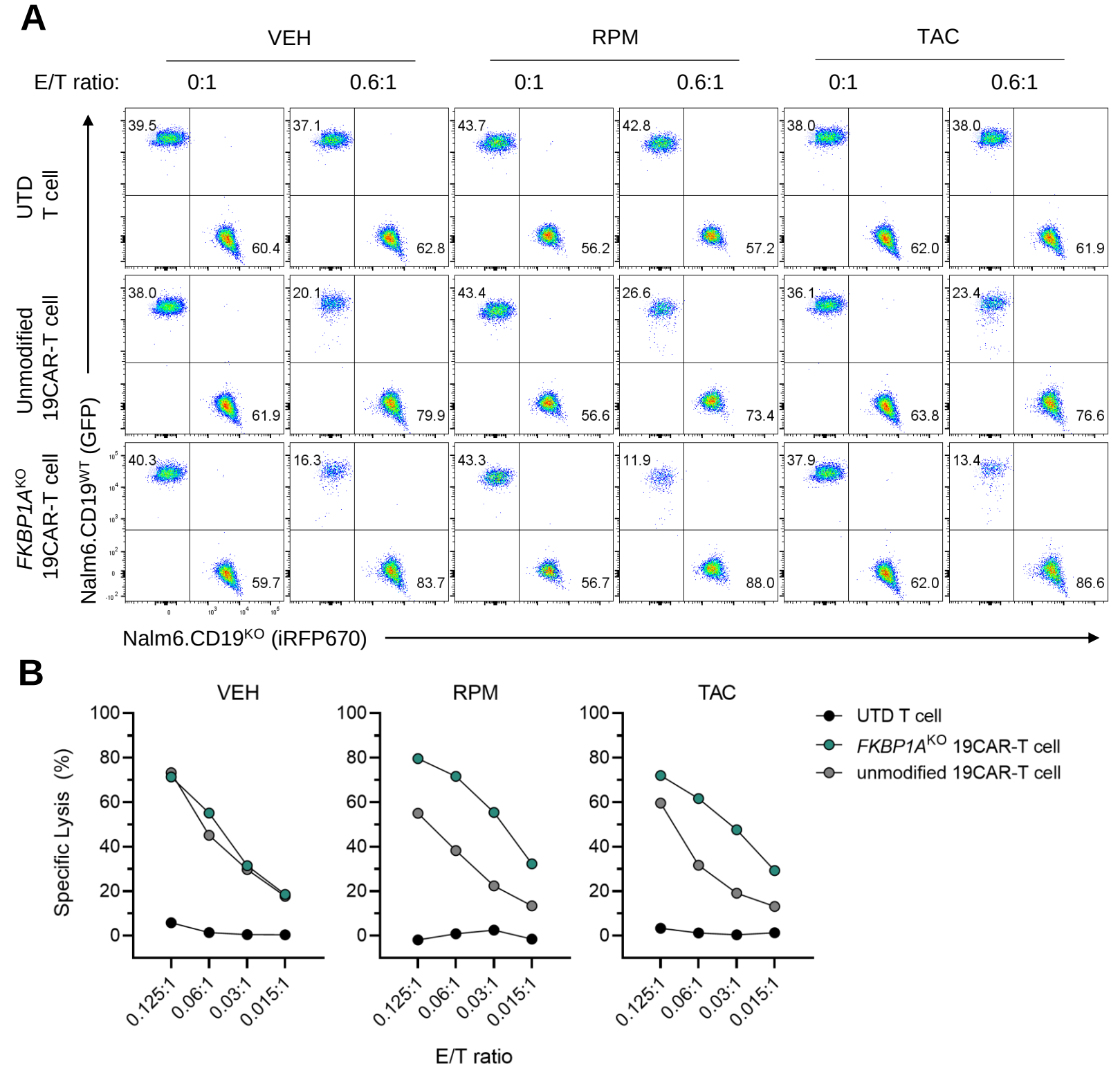

***FKBP1A*^{KO} 19CAR-T cells exhibit *in vitro* anti-tumor cytotoxic activity in the presence of immunosuppressants using VITAL killing assay.** VITAL killing assay as described in Methods. **A** FACS plots indicate frequency of residual on-target Nalm6.CD19^{WT}.GFP^{+} tumor cells and off-target Nalm6.CD19^{KO}.iRFP670^{+} tumor cells at 0:1 and 0.6:1 effector-to-target (E/T) ratio with untransduced (UTD) T cells, unmodified 19CAR-T cells, or *FKBP1A*^{KO} 19CAR-T cells at 48 hours post-culture. Cultures were treated with DMSO vehicle (VEH) control, rapamycin (RPM) or tacrolimus (TAC) at the start of the assay. **B** Summary data indicates frequency of specific lysis at the indicated E/T ratios in VEH-, RPM- and TAC-treated conditions 48 hours post-culture. Symbols represent mean from conditions set-up in duplicate. T cells were generated using an independent donor from Donor #1 and Donor #2 in Figure S11.

Figure S13

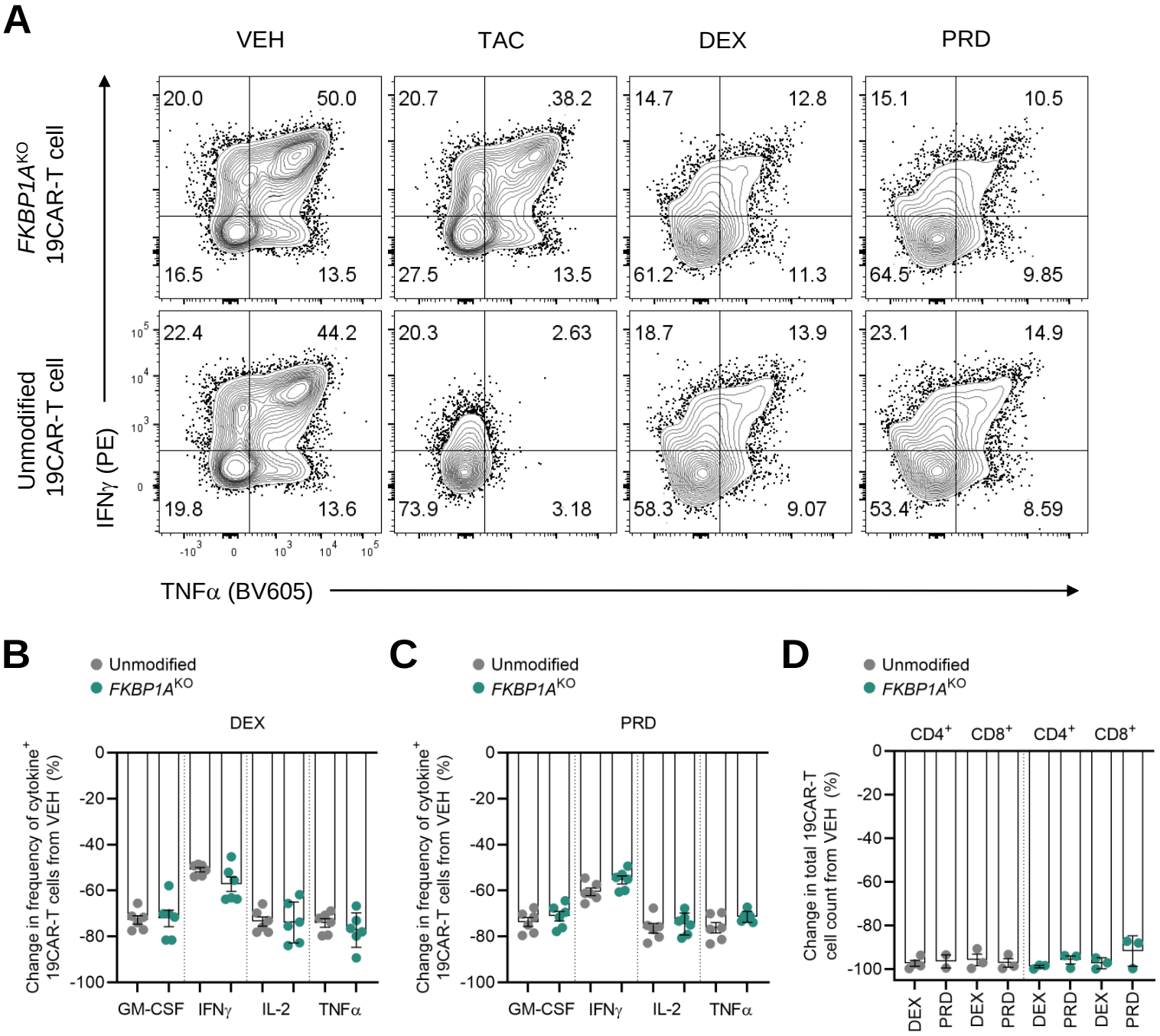

***FKBP1A*^{KO} 19CAR-T cells are sensitive to dexamethasone and prednisone immunosuppression.** Unmodified and *FKBP1A*^{KO} 19CAR-T cells were stimulated with JeKo-1 tumor cells in the presence of DMSO vehicle (VEH) control, tacrolimus (TAC), dexamethasone (DEX) or prednisone (PRD) and then analyzed for intracellular production of cytokines (**A-C**) and proliferation (**D**). FACS plots show frequency of IFNγ and TNFα producing 19CAR-T cells (**A**) and summary data indicates percentage change in frequency of cytokine-positive 19CAR-T cells treated with DEX (**B**) or PRD (**C**) relative to VEH control. Symbols represent 3 independent donors in duplicate. **D** Percentage change in total 19CAR-T cell counts in conditions exposed to DEX or PRD relative to VEH control at 7-days post-stimulation. Symbols represent average of 3 independent donors in triplicate. For all data, bars indicate mean and error bars show ±s.e.m.

Figure S14

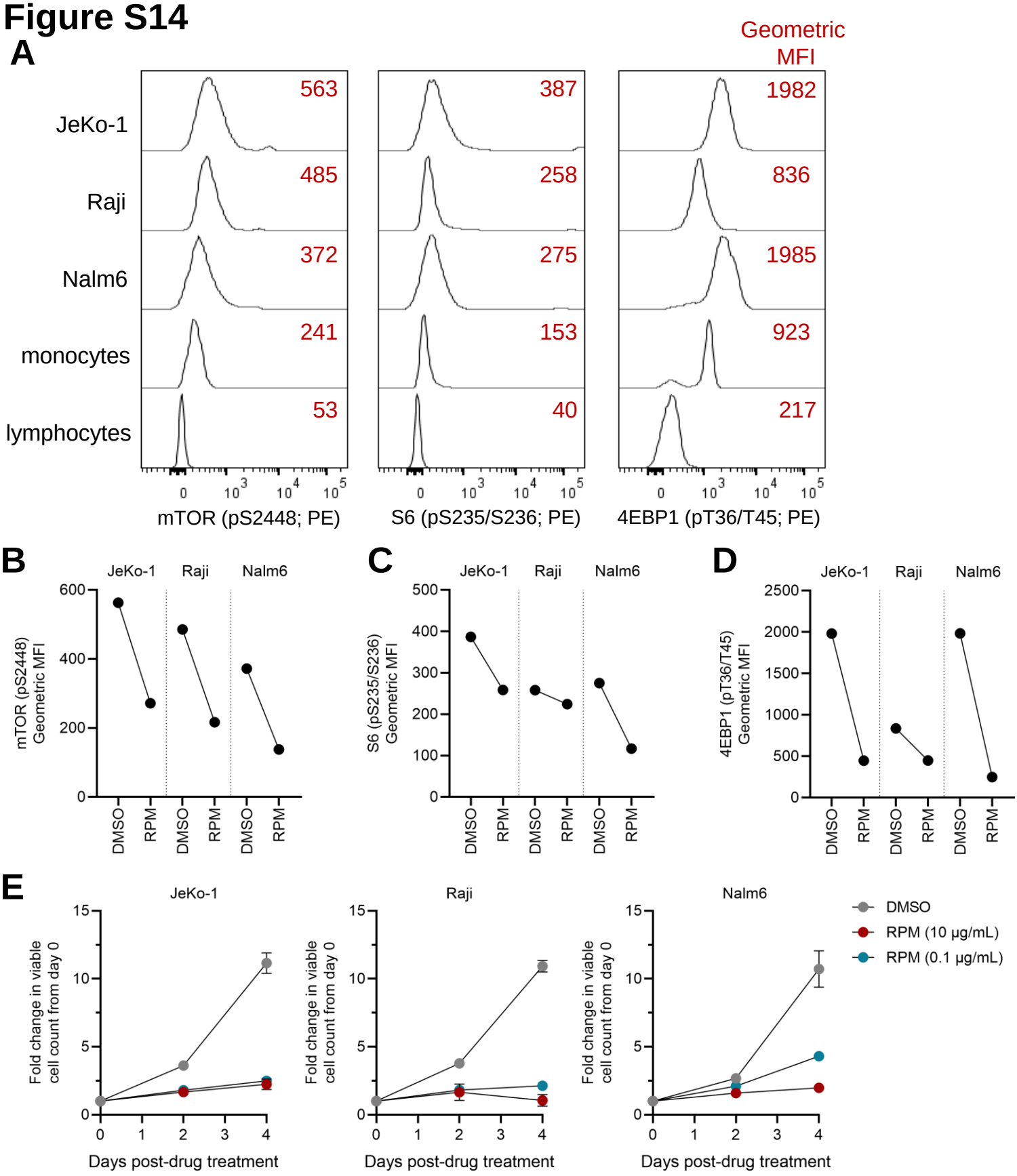

Malignant B cell lines are sensitive to rapamycin treatment *in vitro.* **A** Histograms indicate geometric median fluorescent intensity (MFI) of phosphorylated mTOR (pS2448), S6 (pS235/S2346) and 4EBP1 (pT36/T45) in JeKo-1, Raji and Nalm6 cell lines, as well as primary human monocytes and bulk lymphocytes. **B-D** JeKo-1, Raji and Nalm6 cells were treated with DMSO or rapamycin (RPM) and then analyzed for phosphorylation level of mTOR (**B**), S6 (**C**) and 4EBP1 (**D**). **E** JeKo-1, Raji and Nalm6 cell growth kinetics on 2- and 4-days post-treatment with DMSO or RPM at different drug concentrations. Symbols indicate mean of triplicate samples and error bars show ±s.e.m.

Table S1

Protospacer, base-editor and amplification primers for all target genes

Target Gene	sgRNA ID	Protospacer sequence	Editor (s)	PCR amplification primer (forward)	PCR amplification primer (reverse)
B2M	TSBTx760	CTTACCCCACTTAACTATCT	ABE8.20m	TGTCTTTCAGCAAGGACTGGTCTTTCTA	GACTCATTCAGGGTAGTATGGCCATAGA
B2M	TSBTx845	ACTCACGCTGGATAGCCTCC	rBE4	CGCGCTGGCGGGCATTCCTGAAGCTGA	GCGGGCCACCAAGGAGAACTTGGAGAA
CIITA	TSBTx763	CACTCACCTTAGCCTGAGCA	ABE8.20m / rBE4	ATCACTGACCTGGGTGCCTACAAA	AGAGTTTCTTTCACCACGTCCCGCTAA
CD3E	TSBTx4073	CTGGATTACCTCTTGCCCTC	ABE8.20m	GGATCACCTGTCACTGAAGGAATTTTCA	CGCAAAGACGCCTGGGCACTGTGA
TRAC	TSBTx754	TTCGTATCTGTAAAACCAAG	rBE4	GAGCTGCAGGCCTCCCCCACCCA	GCAGATTAAACCCGGCCACTTTCAGG
FKBP1A	TSBTx1538	CTCACCGTCTCCTGGGGAGA	ABE8.20m	CCGAGGTACTAGGCAGAGC	CCCTGAGGAGACAGAGACGG
FKBP1A	TSBTx1542	ACCGGTGTAGTGCACCACGC	ABE8.20m	CCCAGGAGACGGTGAGTAGT	CCTCGACGGCCAGCC
FKBP1A	TSBTx1545	TACCCAAGAACAGGGAGCTA	ABE8.20m	TATGCCTATGGTGCCACTGG	CTCTGCTACCCATCAAACGC
FKBP1A	TSBTx1546	CCCCAACAGATCTGCCATGG	ABE8.20m	GTCGCCACTGCACACAAAG	TCGGAAGCAAAGCTGAG
FKBP1A	TSBTx1581	TTCACAGGGATGCTTGAAGA	ABE8.20m	TGATGAGTGCTCTGCTGCTG	GAGAGAGCATACCTGGGCAA
FKBP1A	TSBTx1582	CGCCGCCATGGGAGTGCAGG	ABE8.20m	CCGAGGTACTAGGCAGAGC	CCCTGAGGAGACAGAGACGG
FKBP1A	TSBTx1537	CAGGTGGAAACCATCTCCCC	rBE4	CCGAGGTACTAGGCAGAGC	CCCTGAGGAGACAGAGACGG
FKBP1A	TSBTx1538	CTCACCGTCTCCTGGGGAGA	rBE4	CCGAGGTACTAGGCAGAGC	CCCTGAGGAGACAGAGACGG
FKBP1A	TSBTx1539	GCGCCCTGAGGAGACAGAGA	rBE4	CCCAGGAGACGGTGAGTAGT	CCTCGACGGCCAGCC
FKBP1A	TSBTx1540	CGCCCTGAGGAGACAGAGAC	rBE4	CCCAGGAGACGGTGAGTAGT	CCTCGACGGCCAGCC
FKBP1A	TSBTx1541	CAAGCGCGGCCAGACCTGCG	rBE4	CCCAGGAGACGGTGAGTAGT	CCTCGACGGCCAGCC
FKBP1A	TSBTx1542	ACCGGTGTAGTGCACCACGC	rBE4	CCCAGGAGACGGTGAGTAGT	CCTCGACGGCCAGCC
FKBP1A	TSBTx1543	ACTCATCTGTGAAAAGAACA	rBE4	GGCCAAGGAACACCTAGGTA	GAAGCTCCACATCGAAGACG
FKBP1A	TSBTx1544	CGATGTGGAGCTTCTAAAAC	rBE4	TATGCCTATGGTGCCACTGG	CTCTGCTACCCATCAAACGC
FKBP1A	TSBTx1545	TACCCAAGAACAGGGAGCTA	rBE4	TATGCCTATGGTGCCACTGG	CTCTGCTACCCATCAAACGC
FKBP1A	TSBTx1577	AGCAGGAGGTGATCCGAGGC	rBE4	CACAGGGATGCTTGAAGATGG	CACAGGGATGCTTGAAGATGG
FKBP1A	TSBTx1578	GCAGGAGGTGATCCGAGGCT	rBE4	CACAGGGATGCTTGAAGATGG	CACAGGGATGCTTGAAGATGG
FKBP1A	TSBTx1579	GTGATCCGAGGCTGGGAAGA	rBE4	CACAGGGATGCTTGAAGATGG	CACAGGGATGCTTGAAGATGG
FKBP1A	TSBTx1580	GATCCGAGGCTGGGAAGAAG	rBE4	CACAGGGATGCTTGAAGATGG	CACAGGGATGCTTGAAGATGG
CD19	TSBTx3773	CCAGACCTCACCATGGCCCC	ABE8.20m	-	-

Table S2

HLA class-I typing for human allogeneic CAR-T cell donors and HIS mice

Figure	HIS mouse strain	Cohort	HLA class-I typing	Allogeneic T cell donor	HLA class-I typing
1F-H	BLT-NSG	-	A*01:01 A*31:01 B*52:01 B*57:01 C*06:02 C*12:02	DC71	A*02:01 A*24:02 B*17:02 B*15:01 C*03:03 C*05:01
3	BLT-NSG	2	A*68:01:01 A*74:01:01 B*53:01:01 B*58:02:01 C*04:01:01 C*06:02:01	TALL106	A*30*02:01 A*80:01:01 B*18:01:01 B*42:02:01 C*02:02:02 C*17:01:01
3	huNCG	3	A*02:05:01 A*23:17:01 B*15:03:01 B*35:01:01 C*02:10:01 C*04:01:01	D341119	A*01:01:01 A*24:02:01 B*37:01:01 B*39:01:01 C*06:02:01 C*07:02:01
3	huNCG	4	A*01:01:01 A*02:01:01 B*08:01:01 B*35:12:01 C*04:01:01 C*07:01:01	D341119	A*01:01:01 A*24:02:01 B*37:01:01 B*39:01:01 C*06:02:01 C*07:02:01
3	BLT-NSG	5	A*02:01:01 A*23:17:01 B*53:01:01 B*82:02:01 C*04:01:01 C*08:02:01	D341388	A*23:01:01 A*68:01:02 B*44:02:01 B*44:03:01 C*07:04:01 C*07:04:01
6	huNCG	6	A*01:01:01 A*32:01:01 B*08:01:01 B*14:01:01 C*07:01:01 C*08:02:01	CPD-PT060	A*24:02:01 A*68:01:02 B*35:10:00 B*51:01:01 C*03:04:01 C*15:02:01
6	huNCG	7	A*02:01:01 A*02:06:01 B*35:01:01 B*50:02:01 C*06:02:01 C*07:02:01	CPD-PT060	A*24:02:01 A*68:01:02 B*35:10:00 B*51:01:01 C*03:04:01 C*15:02:01
6	huNCG	8	A*02:01:01 A*30:01:01 B*15:01:01 B*38:01:01 C*03:03:01 C*12:03:01	CPD-PT060	A*24:02:01 A*68:01:02 B*35:10:00 B*51:01:01 C*03:04:01 C*15:02:01
6	huNCG	9	A*03:01:01 A*26:01:01 B*27:05:02 B*44:03:01 C*01:02:01 C*16:01:01	CPD-PT060	A*24:02:01 A*68:01:02 B*35:10:00 B*51:01:01 C*03:04:01 C*15:02:01
S1A	BLT-NSG	-	A*02:01 A*30:02 B*18:01 B*45:01 C*05:01 C*16:01	DC70	A*01:01 A*31:01 B*08:01 B*15:17 C*07:01 C*07:01